A Review of Medical Image Segmentation: Methods and Available Software

Daniel J. Withey[a], Zoltan J. Koles[a,b]

[a]*Department of Electrical and Computer Engineering, University of Alberta, Edmonton, Canada*
[b]*Department of Biomedical Engineering, University of Alberta, Edmonton, Canada*

Correspondence: ZJ Koles, Department of Electrical and Computer Engineering, 2nd Floor ECERF, University of Alberta, Edmonton, Alberta, Canada T6G 2V4. E-mail: z.koles@ualberta.ca, phone (780) 492-6302, fax (780) 492-1811

Abstract. Automatic medical image segmentation is an unsolved problem that has captured the attention of many researchers. The purpose of this survey is to identify a representative set of methods that have been used for automatic medical image segmentation over the past 35 years and to provide an opportunity to view the transitions that have occurred as this research area has developed. To facilitate this, the existing research is divided into three generations, each generation adding an additional level of algorithmic complexity. These generations indicate progress towards accurate, fully-automatic, medical image segmentation and their identification provides a framework for classifying the wide variety of methods that have been devised. The first generation is composed of the simplest forms of image analysis such as the application of intensity thresholds and region growing. The second generation is characterized by the application of uncertainty models and optimization methods, and the third generation incorporates knowledge into the segmentation process. The progress toward accurate, fully-automatic segmentation is discussed and sources of segmentation software from industry and academia are identified, along with databases for segmentation validation.

Keywords: Medical Image Segmentation, Medical Image Analysis, Magnetic Resonance Imaging, Computed Tomography.

1. Introduction

Segmentation of structural, medical images is an important step in the formation of realistic tissue models, such as those used in EEG source localization [Michel et al., 2004]. Structural, medical images, can be obtained from magnetic resonance (MR) imaging and X-ray computed tomography (CT), and are commonly held as two-dimensional (2D) arrays of picture elements (pixels) or three-dimensional (3D) arrays of volume elements (voxels, also called pixels). Segmentation is the process of dividing these images into constituent subregions and can be performed by the identification of a surface for each tissue class, or by the classification of each pixel in the image volume. Manual segmentation is possible but is a time-consuming task and subject to operator variability. Reproducing a manual segmentation result is difficult and the level of confidence ascribed to it suffers accordingly. Automatic methods are, therefore, preferable [Clarke et al., 1995]; however, significant problems must be overcome to achieve segmentation by automatic means and it remains an active research area.

Segmentation of medical images involves three main image-related problems. The images may contain *noise* that can alter the intensity of a pixel such that its classification becomes uncertain. Also, the images can exhibit *intensity nonuniformity* where the intensity level of a tissue class varies gradually over the extent of the image. Third, the images have finite pixel size and are subject to *partial volume averaging* where individual pixel volumes contain a mixture of tissue classes so that the intensity of a pixel in the image may not be consistent with any single tissue class.

These image-related problems and the variability in tissue distribution among individuals in the human population means that some degree of uncertainty must be attached to all segmentation results. This includes segmentations performed by medical experts where variability occurs between experts (inter-observer variability) as well as for a given expert performing the same segmentation on multiple occasions (intra-observer variability). Despite this variability, image interpretation by medical experts is generally considered to be the only available truth for in vivo imaging [Clarke et al., 1995].

Medical image segmentation can, therefore, be viewed as an underdetermined problem where the known information is not sufficient to allow the identification of a unique solution. The challenge in developing automatic segmentation methods is in the selection of mathematical models, algorithms, and related parameter values to compensate for the missing detail and produce a solution that is judged to be acceptable by one or more medical experts.

We classify the medical image segmentation literature into three generations, each representing a new level of algorithmic development. The earliest and lowest-level processing methods occupy the first generation. The second is composed of algorithms using image models, optimization methods, and uncertainty models, and the third is characterized by algorithms that are capable of incorporating a priori knowledge. The second generation has followed the first, chronologically, as computing power increased, whereas the third has begun in parallel with the second, often utilizing methods from the first and second generations. These generations indicate progress toward accurate, fully-automatic medical image segmentation and their identification provides a framework for classifying the wide variety of methods that have been devised.

We focus primarily on the segmentation of 2D and 3D MR and CT images of the human head although many of the methods can also be applied to other image types and to images from other modalities.

Automatic segmentation methods have been previously classified as either *supervised* or *unsupervised* [Bezdek et al., 1993]. Supervised segmentation requires operator interaction throughout the segmentation process whereas unsupervised methods generally require operator involvement only after the segmentation is complete. Unsupervised methods are preferred to ensure a reproducible result [Clarke et al., 1995]; however, operator interaction is still required for error correction in the event of an inadequate result [Olabarriaga and Smeulders, 2001].

Also, objects within the images can be identified either by labeling all pixels in the object volume, or by identifying boundaries of the objects. Some segmentation methods may also be categorized in this manner, as *volume identification* methods or as *boundary identification* methods.

Most publications concern segmentation of magnetic resonance (MR) images as opposed to CT images. More soft tissue detail is possible with MR imaging, and multispectral images, each with different relative tissue intensity levels, can be obtained in a single acquisition session. Multispectral images are often used in segmentation methods based on clustering or other pattern recognition techniques.

The number of publications regarding medical image segmentation is quite large and as a result the following information is intended to be representative rather than exhaustive. Previous review articles [Bezdek et al., 1993; Clarke et al., 1995; McInerney and Terzopoulos, 1996; Bezdek et al., 1997; Jain et al., 1998; Duncan and Ayache, 2000; Haacke and Liang, 2000; Jain et al., 2000; Pham et al., 2000; Montagnat et al., 2001; Olabarriaga and Smeulders, 2001; Suri et al., 2002a; Suri et al., 2002b; Angenent et al., 2006] and references cited in the text are sources for related articles and additional details.

The remainder of this review is organized as follows. The three generations of medical image segmentation are identified along with a representative set of examples for each. This is followed by a description of available segmentation software and of available, on-line image databases having ground truth segmentations suitable for algorithm evaluation. Finally, the segmentation methods are summarized and the progress of automatic medical image segmentation toward equivalence with human-expert segmentation is discussed.

2. First Generation

The first generation includes low-level techniques applied by an operator to create one-time, ad hoc segmentations and low-level techniques that utilize heuristics. The application details (e.g. threshold levels, homogeneity criterion) are determined by the operator. Simple methods like these are subject to all three of the main image segmentation problems. Further description can be found in textbooks on image processing (e.g. Pratt (1991), Pitas (1993), Weeks (1996), and Nikolaidis and Pitas (2001)).

2.1. Thresholds

A threshold can be applied to an image to distinguish regions with contrasting intensities and thus differentiate between tissue regions represented within the image. But, in images where intensity nonuniformity and noise are present it may be difficult or impossible to find one or more thresholds to segment the image without serious misclassification. The application of thresholds is extremely simple

and they continue to be used when the nature of the problem permits or when augmented by additional processing steps.

2.2. Region Growing

Starting at a seed location in the image, adjacent pixels are checked against a predefined homogeneity criterion. Pixels that meet the criterion are included in the region. Continuous application of this rule allows the region to grow, defining the volume of an object in the image by identification of similar, connected pixels.

Region growing continues to be used where the nature of the problem permits and developments continue to be reported [Hojjatoleslami and Kittler, 1998; Hojjatoleslami and Kruggel, 2001; Wan and Higgens, 2003].

2.3. Region Split/Merge

The region split/merge segmentation algorithm (e.g. see Nikolaidis and Pitas (2001)) operates on an image in a recursive fashion. Beginning with the entire image, a check is performed for homogeneity of pixel intensities. If it is determined that the pixels are not all of similar intensity then the region is split into equal-sized subsections. For 3D images, the volume is split into octants (quadrants for 2D images) and the algorithm is repeated on each of the subsections down to the individual pixel level. This usually results in over-segmentation where homogeneous regions in the original image are represented by a large number of smaller subregions of varying size. A merge step is then performed to aggregate adjacent subregions that have similar intensity levels.

2.4. Edge Tracing

Edge detection, a commonly used image processing technique, is typically not suitable for image segmentation on its own since the edge pixels identified are based on local intensity variations and are not necessarily well-connected to form closed boundaries [Haacke and Liang, 2000; Nikolaidis and Pitas, 2001]. However, edge detection can be used to supplement other segmentation techniques.

Edge tracing is a boundary identification method where edge information is extracted and edge pixels with adjacent-neighbour connectivity are followed sequentially and collected into a list to represent an object boundary [Martelli, 1976; Lineberry, 1982; Pitas, 1993]. Evaluation of a cost function, possibly involving a variety of local and global image features, is performed in the search for neighbouring pixels. The application of heuristics, for algorithmic simplicity and to reduce computation time, can produce suboptimal results. Additionally, these algorithms tend to be very sensitive to noise that creates gaps or diversions in the object boundary. Methods for extracting 3D surfaces, by stacking 2D contours [Cappelletti and Rosenfeld, 1989] and by a 3D edge following procedure [Qu and Li, 1996], have also been developed.
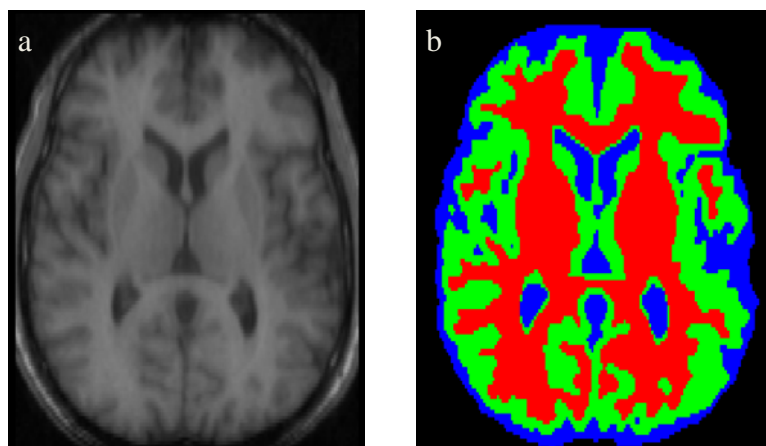

Figure 1.   *a) Slice of a 3D volume; and, b) Segmentation result using a statistical pattern recognition method. Red corresponds to white matter, green to gray matter and blue to cerebrospinal fluid. (FAST segmentation from FSL, MR image from IBSR.)*

3. Second Generation

Research in automatic image segmentation diverges from the first-generation algorithms with the introduction of uncertainty models, reliance on optimization methods, and a general avoidance of heuristics. Segmentation methods can often still be identified as being primarily one of either volume identification or boundary identification and as either supervised or unsupervised.

3.1. Statistical Pattern Recognition

Statistical pattern recognition [Bezdek et al., 1993; Jain et al., 2000] has been applied extensively in medical image segmentation. A mixture model is used where each of the pixels in an image is modeled as belonging to one of a known set of classes. For head images, these will be tissue classes such as gray matter, white matter, and cerebrospinal fluid. A set of features, often involving pixel intensity, is evaluated for each pixel. This forms a set of patterns, one for each pixel, and the classification of these patterns assigns probability measures for the inclusion of each pixel in each class.

As part of the process, class conditional probability distributions describing the variation of each pixel feature are often required for each class. These are generally not known and can be determined manually or automatically. For example, in supervised, statistical classification these distributions can be calculated from operator-selected regions acquired from each tissue class in the image. Alternatively, in unsupervised, statistical clustering, the distributions are automatically estimated from the image data, usually requiring an iterative procedure.

The total number of classes present in the image and the a priori probability of occurrence of each class within the image are assumed to be known prior to the segmentation operation. For each pixel in the input image, the a posteriori probability that the pixel belongs to each tissue class is generally computed using Bayes' rule [Bezdek et al., 1993] and a maximum a posteriori (MAP) rule is applied, where the pixel is assigned to the class in which its a posteriori probability is greatest, to complete the segmentation.

Parametric approaches in statistical pattern recognition are those where the forms of the class conditional distributions are known, as, for example, when Gaussian distributions are assumed, and nonparametric approaches are those where the forms of the class conditional distributions are not known. Certain nonparametric approaches (e.g. k-Nearest Neighbour classifier) do not require class conditional distributions.

Bayesian classifiers [Bezdek et al., 1993], discriminant analysis [Amato et al., 2003], maximum likelihood [Clarke et al., 1993] and k-Nearest Neighbour classifiers [Bezdek et al., 1993; Clarke et al., 1993; Anbeek et al., 2005] are examples of methods that have been applied in supervised segmentation.

Unsupervised, volume identification has been performed using parametric, statistical clustering implemented with expectation maximization (EM), a two-step, iterative procedure, and where a mixture of Gaussians is assumed for the pixel intensity data. This has allowed segmentation and nonuniformity gain field estimation to occur simultaneously [Wells et al., 1996; Held et al., 1997; Van Leemput et al., 1999], addressing the intensity nonuniformity problem.

The application of a Markov random field (MRF) [Chellappa and Jain, 1993] to introduce contextual information by allowing neighbour pixels to influence classification and by modeling a priori information regarding the possible neighbours for each tissue class, has helped to reduce misclassification errors arising from noise and partial volume averaging [Held et al., 1997; Van Leemput et al., 1999]. An extension to further address the partial volume problem is found in Van Leemput et al. (2003). A generalization of the EM-MRF approach which uses a hidden Markov random field and EM is reported by Zhang et al. (2001). This method has been used to form the segmentation shown in Fig. 1.

A computationally efficient method for automatically determining the MRF control parameter which determines the amount of spatial regularization is described by Woolrich and Behrens (2006). A segmentation method using a variant of the EM algorithm and which estimates a separate bias field for each tissue class is described by Marroquin et al. (2002). The relatively high computational cost of the EM approach, though, has spurred the search for speed enhancements [Ng and McLachlan, 2004; M'hiri et al., 2007] and alternatives [Marroquin et al., 2003].

Statistical models to describe partial volume averaging have been developed, for example that of Tohka et al. (2004) and also González Ballester et al. (2002), where a statistical representation for the volume of the segmented object is also computed.

3.2. C-means Clustering

C-means cluster analysis [Bezdek et al., 1993] permits image pixels to be grouped together based on a set of descriptive features. For example, intensity could be used as a feature, causing pixels to be grouped according to intensity levels. Other features which describe individual pixels (e.g. the texture of a local neighbourhood) can also be used to improve cluster separation. The numerical value of each feature is generally normalized to between 0 and 1.

C-means cluster analysis operates in the *p*-dimensional feature space, where *p* is the number of features used. Each pixel produces one point in the feature space and a cluster is a region in the feature space having a high density of such points. For each cluster, a cluster centre, or prototype, can be defined. The membership of a pixel in a particular cluster depends on the distance between its feature-space representation and the cluster prototypes.

The number of clusters, c, is assumed to be known. Equations for iterative computation of the positions of the cluster prototypes and the memberships of each pixel in a cluster are determined by minimizing an objective function based on the sum of the distances (i.e. some measure of similarity) between the cluster prototypes and each of the *p*-dimensional data points. During algorithm operation, there is no guarantee that a global minimum will be attained. The algorithm execution is terminated when the first local minimum is reached.

Hard c-means algorithms assign to each pixel absolute membership in one of the clusters whereas fuzzy c-means algorithms assign to each pixel a degree of membership within each of the clusters. Hardening of the fuzzy result is often done by assigning each pixel to the cluster in which it has highest membership.

Adaptive methods based on fuzzy c-means clustering (FCM) have been used for unsupervised, volume identification [Pham and Prince, 1999; Pham, 2001]. The adaptive technique is implemented by modifying the FCM objective function and provides compensation for the intensity nonuniformity problem. Alternatives that reduce computational complexity and add spatial constraints, for reduction of errors due to noise, have also been reported [Ahmed et al., 2002; Liew and Yan, 2003; Zhang and Chen, 2004].
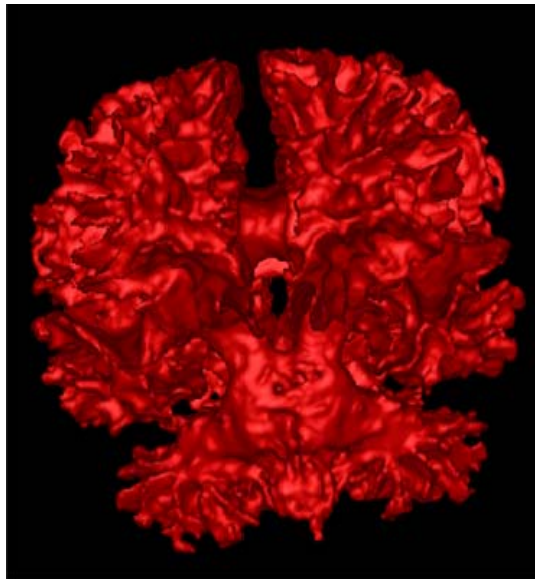

Figure 2. *3D visualization of a brain white matter surface produced by a level set-based deformable model. (Formed with the SNAP segmentation application, MR image from IBSR.)*

3.3. Deformable Models

Deformable models, including active contours (2D) and active surfaces (3D), are artificial, closed contours/surfaces able to expand or contract over time, within an image, and conform to specific image features.

One of the earliest active contours is the snake [Kass et al., 1988], used for supervised, boundary identification in 2D images. The snake is endowed with physical elasticity and rigidity features and intensity gradients in the image are used to derive external forces acting on the snake. During iterative

update of an energy-minimization evolution equation, the snake moves to the nearest edge and is able to conform to it, identifying the boundary of an object within the image.

In the early stages of development, the snake needed to be initialized very near to the boundary of interest, had difficulty entering narrow concavities, and had problems discriminating between closely spaced objects. Attempts to overcome these problems resulted in many modifications [McInerney and Terzopoulos, 1996]. Extensions to allow 3D volume segmentation were also developed as was the ability to change topology to handle objects with bifurcations or internal holes [McInerney and Terzopoulos, 1996; McInerney and Terzopoulos, 1999]. New snake models continue to be developed [Xu and Prince, 1998, Meegama and Rajapakse, 2003; Wang and Li, 2003; Wei et al., 2004; Li and Acton, 2007; Sum and Cheung, 2007].

Level-set methods were introduced to deformable models by casting the curve evolution problem in terms of front propagation rather than energy minimization [Malladi et al., 1995; Caselles et al., 1997a,b; Sethian, 1999]. With level sets, the contour or surface moves in the direction of its normal vectors. The speed of the contour is an important component for maintaining consistent contour propagation and for halting at regions of high gradient. Local contour curvature, intensity gradient, shape, and contour position can be used in the speed term although the selection need not be limited to these [Sethian, 1999]. The development of the level set approach simplified topology adaptation so that a contour or surface could split and merge as it evolved, allowing it to identify boundaries of complex objects. A topology-preserving level set method has also been developed where the topology of the final surface matches that of the initial surface [Han et al., 2003]. Efforts have also been made to reduce the computational burden [Xu et al., 2004]. The segmentation shown in Fig. 2 was performed using a level-set algorithm.

Mumford-Shah segmentation techniques [Mumford and Shah, 1989], rather than intensity gradient, have been used to form the stopping condition [Chan and Vese, 2001] producing a region-based, active contour and this has been further developed to produce a deformable model that finds multiple object boundaries with simultaneous image smoothing [Tsai et al., 2001]. Mumford-Shah segmentation assumes a piecewise smooth image representation and defines a problem in variational calculus where the solution produces simultaneous smoothing and boundary identification in an image [Mumford and Shah, 1989].

The application of radial basis functions collocation, as an alternative to the usual finite-difference solution of the underlying level-set evolution partial differential equation (PDE), has been reported. Benefits include propagation constraints and the smoothness and continuity of the solution [Gelas et al., 2007].

Most deformable models propagate toward a local optimum and thus exhibit sensitivity to initial conditions. Work to develop globally optimal active contours has been performed [Bresson et al., 2007]. A method for finding globally optimal surfaces by simulating an ideal fluid flow under image-derived, velocity constraints is described by Appleton and Talbot (2006).

3.4. Graph Search

For image analysis, a graph is constructed from an image where image pixels become nodes in the graph and the nodes are interconnected to neighbouring nodes, mapping the corresponding pixel associations in the image. The interconnections can be directed, where there is an implied direction for transitioning from one node to another, or undirected. Costs for each interconnection are determined based on a cost function which can include both boundary and region components. Minimum-cost solutions to the problems of boundary identification and object volume identification are obtained using algorithms from combinatorial optimization.

Graph searching has been applied to form optimal edge-linking strategies in a supervised, boundary-identification method known as "Live Wire" [Barrett and Mortensen, 1997; Falcão et al., 1998; Falcão et al., 2000]. An initial seed pixel and a destination pixel are specified and the cost for transfer between pixels in the intervening trellis is computed based on a given cost function. The minimum-cost path between the initial pixel and the destination pixel can then be determined and the pixel sequence collected into a list. Repetition of this procedure where each destination pixel is used as the initial pixel in a subsequent operation allows an operator to guide the formation of an object boundary. Dynamic programming is used for determining the minimum-cost path [Falcão et al., 1998]. An extension to permit user-guided, 3D boundary formation has also been developed [Falcão and Udupa, 2000].

A graph cut is a set of interconnections between nodes in a graph which, when removed, partition the graph into two distinct sets. The sum of the costs of the graph cut is the cost of the cut. Minimal-cost cuts are desired and produce a globally-optimal segmentation of the graph which, given

appropriate interconnection costs, identifies an object from its background in the image. Graph cuts are related to active contours and level sets, among the deformable models, which are their continuous-space analogs [Boykov and Funka-Lea, 2006]. Whereas most deformable models propagate toward a local optimum, graph cuts produce globally-optimal boundaries with an attendant advantage in robustness. Graph cuts can be used for surface identification in N-dimensional images [Boykov and Funka-Lea, 2006].

A generalization unifying all optimal, graph-search algorithms is provided by Falcão et al. (2004).

Fuzzy Connectedness

Fuzzy representations of connectedness between the pixels comprising an object in an image, drawn from early work on fuzzy image analysis by Rosenfeld [Rosenfeld, 1983; Rosenfeld, 1984], have been developed for use in medical image segmentation [Udupa and Samarasekera, 1996; Udupa and Saha, 2003]. Given a seed pixel within an object in an image, the object containing the seed is determined by computing a connectedness measure for all pixels in the image relative to the seed pixel. Final object selection is performed using a threshold on the resulting fuzzy connectedness map. When multiple objects are considered, a seed pixel is required for each object and the fuzzy connectedness of all image pixels to each seed are computed. Pixels are then assigned to the object of highest connectedness. Intensive computation may be required because connectedness is defined based on an optimal path to the seed pixel. Dynamic programming is used to determine the optimal paths.

Fuzzy connectedness has been used in intra-operative tumour segmentation where a rectangular, operator-selected region of interest surrounding the tumour has also been applied to reduce computation time [Hata et al., 2005]. Fuzzy connectedness is closely related to other graph-search algorithms [Falcão et al., 2004].

Watershed Algorithm

The watershed algorithm is a boundary identification method in which gray-level images are modeled as topographic reliefs where the intensity of a pixel is analogous to the elevation at that point [Vincent and Soille, 1991]. In a real landscape, catchment basins, e.g. lakes and oceans, are regions each associated with a local minimum. In a similar way, a gray-level image has local minima. The watershed concept can be understood by imagining that a hole is cut at each local minimum in the relief and then the relief is immersed, minima first, into water. As the relief is immersed, water rises from the holes in the local minima. At each point where water would flow from one catchment basin to another, a "dam" is constructed by marking those points. When the entire relief has been immersed in water, the "dams" ring each catchment basin in the image, identifying the boundaries of the local minima. The tendency is to oversegment the image since every local minimum will be identified including those resulting from noise. Thresholds are generally used to suppress shallow minima. Often edge detection is used to produce a gradient magnitude image for input to the watershed algorithm since the catchment basins will then be the objects of interest, that is, regions not associated with edges in the image. The watershed algorithm has been classified as a graph-search algorithm [Falcão et al., 2004].

3.5. Neural Networks

Artificial neural networks have been used in medical image segmentation [Bezdek et al., 1993], typically in unsupervised, volume identification but also in boundary identification [Barrios et al., 1994]. The network must first be trained with suitable image data, after which it can be used to segment other images. For volume identification, the neural network acts as a classifier where a set of features is determined for each image pixel and presented as input to the neural network. The network uses this input to select the pixel classification from a predefined set of possible classes, based on its training data. The classification operation is like that performed in statistical pattern recognition and it has been noted that many neural network models have an implicit equivalence to a corresponding statistical pattern recognition method [Jain et al., 2000].

Investigations of biological neurons in animal models have shown that neurons of the visual cortex produce stimulus-dependent synchronization [Eckhorn, 1999]. This has led to the suggestion that the synchronous activity is part of the scene segmentation process. Neural networks have been formed using artificial neurons derived, with significant simplification, from the physiological models and used for unsupervised, volume identification. Examples are pulse coupled neural networks (PCNNs) [Johnson and Padgett, 1999] and the locally excitatory globally inhibitory oscillator network (LEGION) [Shareef et al., 1999]. The artificial neurons are usually arranged in a one-to-one correspondence to the image pixels and have linkages to a neighbourhood of surrounding neurons.

Each neuron produces a temporal pulse pattern that depends on the pixel intensity at its input and also on the local coupling. The linkages between neurons permit firing synchrony and the time signal from a group of neurons driven by the same object in an image is specific to that object. The local coupling helps to overcome intensity nonuniformity and noise. Implementations of PCNNs as hardware arrays have been considered, with the intent of producing real-time, image-processing systems [Johnson and Padgett, 1999].

Unsupervised, volume identification has also been performed by a method utilizing vector quantization and a deformable feature map where training required one manually segmented dataset [Wismuller et al., 2004].

Neural networks have also been used as an autoassociative memory to identify lesions [Raff and Newman, 1992]. The network is trained using images from normal subjects. When an image containing an abnormality is presented to the network, the abnormality is recognized as different from the training images.

Neuro-fuzzy systems, combinations of neural networks and fuzzy systems, have also been used in image segmentation. Boskovitz and Guterman (2002) provide a brief survey and propose a system which performs image segmentation by neural network-controlled, adaptive thresholds applied to a "fuzzified" version of the input image obtained by fuzzy clustering.

3.6. Multiresolution Methods

Multiresolution, multiscale, and pyramid analysis are terms referring to the use of scale reduction to group pixels into image objects. These methods are typically used for unsupervised, volume identification but have also been used in unsupervised, boundary identification. The segmentation is performed by first forming a set, or stack, of images by recursively reducing the scale of the original image by blurring followed by down sampling. The result is a sequence of images that if stacked one above the other from highest resolution to lowest resolution would form a pyramid of images, each determined from the one below. The lowest resolution image (apex of the pyramid) may be as small as 2x2x2 pixels, for 3D images, and the highest resolution image (base of the pyramid) is the original. The pixels are then linked from one layer to the next by comparing similarity attributes, such as intensity features. Pixels that have similar features and location are labeled as belonging to the same object, completing the segmentation.

Simple edge tracing methods have been augmented by further processing using multiresolution pyramids to connect edge discontinuities [Soltanian-Zadeh and Windham, 1997] and boundaries have been refined using a multiscale approach [Raman et al., 1991]. Vincken et al. (1997) and Neissen et al. (1999) give examples of volume identification using multiresolution pyramids.

3.7. Geodesic Minimal Path

Unsupervised, boundary identification by edge following has been performed by computing geodesic contours, as used in deformable models based on the methods of level sets [Cohen and Kimmel, 1997]. A geodesic contour is defined as the shortest line on a surface between two points on the surface. Minimal paths are determined by minimizing a weighted distance measure that is lowest along high-intensity gradients in the image Computation involves the numerical solution of partial differential equations. The minimal-path approach described by Cohen and Kimmel (1997) has also been extended to 3D surface extraction. An initialization step to define two constraining contours is required and the final surface contains all minimal paths between the two constraining contours [Ardon et al., 2007].

User-guided, edge following in 2D images has also been implemented using geodesic contours where minimal paths are determined between a series of consecutively-placed, user-defined, boundary points [Chung and Sapiro, 2000].

3.8. Target Tracking

Automatic, target-tracking algorithms employing the discrete Kalman filter for automatic, recursive boundary estimation from edge data have been applied to edge following [Abolmaesumi and Sirouspour, 2004; Withey, 2006]. An example is shown in Fig. 3. Target tracking algorithms are notable for their data fusion capabilities, integration of information from a variety of sources.

3.9. Method Combinations

Examples of combining second-generation, volume identification with second–generation, boundary identification are: multiresolution concepts with watershed algorithm [Letteboer et al., 2004], neural network classification and active contours [Middleton and Damper, 2004], fuzzy clustering and

an active contour method [Amini et al., 2004], statistical methods and active contours [Kapur et al., 1996; Ashton et al., 1995; Chakraborty et al., 1996].

A combination of two boundary identification methods, snakes and Live Wire, the graph-search method of Falcão et al. (1998), was proposed for supervised, boundary identification [Liang et al., 2006]. The Live Wire methods are used for snake initialization and to interactively introduce hard constraints on the snake evolution.
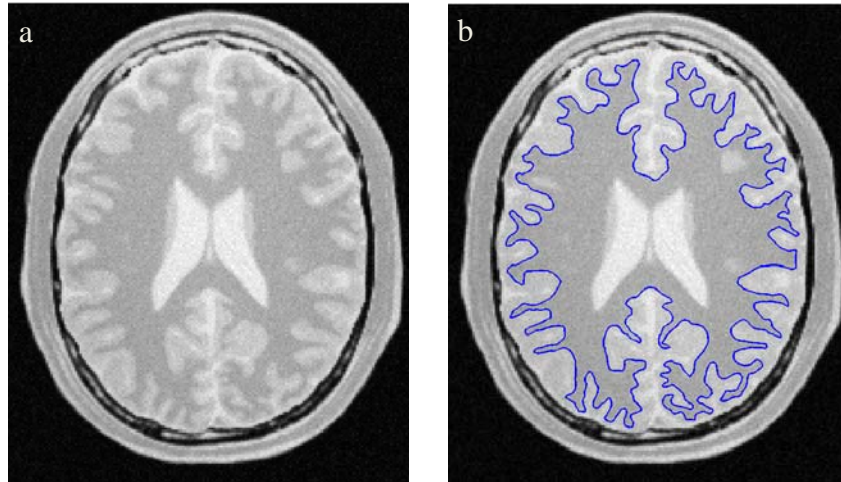

Figure 3. *Result from an edge-tracing segmentation method based on statistical target tracking. a) Original image; b) Image with automatically-delineated tissue boundary. (MR image from MNI brainweb.)*

4. Third Generation

It is important to recognize that medical image segmentation is a challenge even for human experts who have knowledge, training, and awareness at a level that has not been replicated in computer programs. Furthermore, trained experts may disagree on details regarding a particular segmentation [Clarke et al., 1995]. This suggests very strongly that the problem of accurate, fully-automatic image segmentation will not be solved by a second-generation algorithm and that while optimization methods and uncertainty models are important and should be used, they are not sufficient in themselves to produce accurate, automatic segmentations, in the general case. Recent work has led to the development of methods that incorporate higher-level knowledge such as a priori information, expert-defined rules, and models (e.g. shape) of the desired object. These constitute the third generation of medical image segmentation methods.

4.1. Atlas-based Segmentation

An atlas is a segmented image of a single individual, or, a composite head image formed from segmented, co-registered head images of several subjects. In the latter case, a probabilistic atlas is formed and provides information on population variability. Several types are possible, including:
1) an average intensity atlas where each pixel value is determined from its average across all subjects; 2) a tissue type atlas where each pixel contains the probability of belonging to each of a set of tissue classes; and, 3) a structure atlas where the atlas contains the distributions of several structures of interest, as determined from the subject segmentations [Shattuck et al., 2008]. The use of probabilistic atlases has permitted segmentation of the entire brain, including subcortical structures [Fischl et al., 2002]. A detailed example of probabilistic atlas formation is given by Shattuck et al. (2008) and a variety of atlases can be obtained online from http://www.loni.ucla.edu/Atlases/.

Single-subject atlases have been used for segmentation-by-registration where a 3D mapping is determined between the atlas and an unsegmented image and the labeling found in the atlas is used to identify the labeling applied to complete the segmentation [Collins et al., 1995; Dawant et al., 1999].

Probabilistic atlases have been used to improve the selection of a priori probabilities for statistical pattern recognition [Ashburner and Friston, 1997; Van Leemput et al., 1999; Marroquin et al., 2002]. A mapping between the atlas and the unsegmented image is determined by a registration step (warping) and the atlas provides prior probabilities for the pattern recognition algorithm. In a further

development, the required registration step has been incorporated into a statistical clustering framework that also performs simultaneous intensity nonuniformity correction. The expectation-maximization method is used for parameter estimation and the model assumes that the pixel intensities are drawn from a mixture of Gaussians [Ashburner and Friston, 2005]. In most cases, the use of an atlas requires distinct steps for registration and for segmentation. A method for performing atlas registration and segmentation jointly has also been reported [Pohl et al., 2006].

Nonparametric classifiers, where no assumptions are made regarding the pixel intensity distributions, have also been used with atlases [Cocosco et al., 2003; Kim et al., 2005; Jiménez-Alaniz et al., 2006; Vrooman et al., 2007].

Results from a number of single-subject atlases have been combined by first registering each with the unsegmented image to produce a set of possible segmentations. The modal value of the distribution of the assignments for each pixel is used to form the final segmentation. A model for predicting the improvement in segmentation given the number of atlases is also provided [Heckemann et al., 2006].

Atlas-based statistical pattern recognition has been enhanced to include a model of the MR image formation process in order to reduce sensitivity to the image acquisition parameters. The integration of image acquisition into the process also facilitates the derivation of MR imaging sequences that are optimal for the purposes of segmentation [Fischl et al., 2004].

Although fully-automatic registration is desirable, semiautomatic registration is also used where manually-defined landmark points constrain the deformation and improve segmentation accuracy especially in cortical regions where substantial inter-subject variability exists [Dade et al., 2004].

In a manner analogous to probabilistic atlases, fuzzy templates have been formed and used for segmentation of subcortical brain structures [Zhou and Rajapakse, 2005].

The use of an atlas does not necessarily produce superior performance when compared with other segmentation approaches. For example, in at least one comparison that included atlas-based methods, the second-generation, statistical-clustering method of Zhang et al. (2001) was judged to have best overall performance, although most methods in the evaluation performed well [Bouix et al., 2007]. It should also be noted that this comparison involved identification of three tissue classes, gray matter, white matter, and cerebrospinal fluid and did not attempt to identify subcortical structures, where atlas-based methods would be expected to excel.

Atlases have been incorporated into many other algorithms, for example, to enhance edge tracing for supervised, boundary identification in 2D image slices [Färber et al, 2007], to improve fuzzy connectedness segmentation [Zhou and Bai, 2007], in neural network-based classification algorithms [Magnotta et al., 1999; Powell et al., 2006], and also in fuzzy c-means classification [Bazin and Pham, 2007b].

4.2. Rule-based Segmentation

Automatic, rule-based guidance of unsupervised image segmentation has been explored in an attempt to improve the results from unsupervised segmentation methods and yet maintain an automated approach to the segmentation task. Image primitives are usually derived from first-generation and second-generation algorithms and then interpreted using anatomical and image knowledge applied as a set of rules. The wide variety of methods that have been developed can usually be categorized by the types of image information that are extracted, by the types of knowledge that are introduced, and by the method used for implementation of that knowledge.

First-generation methods were often used in early, rule-based systems for image data extraction [Raya, 1990; Ehricke, 1991; Natarajan et al., 1991; Suzuki and Toriwaki, 1991; Li et al., 1995] and although these are relatively simple, low-level processing methods, the methods used for interpretation are not necessarily so. An oversegmented image and a rule-based merging algorithm is used by Natarajan et al. (1991) to segment the lateral ventricles and left caudate nucleus in CT images of the brain. The process incorporates high-level domain knowledge, including an anatomical model.

A brain model describing the structures and features in each 2D slice of a 3D image for object recognition in CT images is described by Li et al. (1995). The method includes a blackboard, that is, a temporary database containing prior and current information that is updated as the segmentation proceeds, and also utilizes data fusion, the combination of multiple data sources to improve decision confidence.

More recently, Xia et al. (2007) describe a system that uses region growing and anatomical knowledge to identify the caudate nucleus from T1-weighted MR images.

Second-generation methods have also been used to extract image primitives for rule-based systems [Sonka et al., 1996; Chen et al., 1998; Clark et al., 1998; Solaiman et al., 1999; Barra and Boire, 2001; Algorri et al., 2004]. An automatic system for segmentation and labeling of glioblastoma-multiforme

tumours in MR images where gadolinium had been used as a contrast agent is described by Clark et al. (1998) with further evaluation by Mazzara et al. (2004). Adaptive thresholds, fuzzy c-means clustering, and a rule-base built from a set of training images are key components of the multistage system. All steps in the system are performed automatically.

Knowledge of anatomical shapes and relative object locations along with a hypothesize-and-verify approach driven by a genetic algorithm has been used to identify basal nuclei, ventricles, and other substructures in 2D, MR, brain images [Sonka et al., 1996].

Possibilistic clustering, a generalization of fuzzy c-means clustering, and fuzzy logic have been used to segment the thalamus, putamen, and the head of the caudate nucleus from brain images of healthy volunteers [Barra and Boire, 2001]. The features used in the clustering process consist of a set of 3D wavelet coefficients extracted from the MR image at each pixel. The clustering is followed by a fuzzy logic step to refine the segmentation by incorporating linguistic descriptions, obtained from a human expert, describing object position and features.

Pitiot et al. (2004) describe a system where a set of mesh surfaces are simultaneously deformed, guided by a series of rules based on the dynamics of the evolving surfaces and on medical knowledge of the shape and texture of the objects of interest. The rules are implemented as constraints on the surface deformation.

4.3. Coupled Surfaces

The simultaneous identification of multiple surfaces with a known spatial relationship has been used to improve segmentation using deformable models [Zeng et al., 1999] and graph-cut methods [Li et al., 2006].

4.4. Shape Models

Statistical, model-based segmentation with nondeformable, shape models was explored as a guide to segmentation by region growing [Arata et al., 1995] but the use of deformable shape models increased greatly in popularity after the development of the active shape model (ASM) [Cootes et al., 1995]. This was inspired by active contours but with the added intention of limiting the extent of the model deformation to within reasonable limits for a given class of object. Since objects of a given class display shape variability, a point distribution model (PDM) is formed using points attached to specific landmarks on a particular object. In the PDM, each landmark point has a statistical distribution determined from a set of N co-registered, example objects, ideally describing the full range of shape variability. Assuming 2D coordinates and n landmark points in the PDM, the ASM can be viewed as a point cloud of N points in a $2n$-dimensional space. A mean contour is determined and the deviation from the mean is computed for each of the N contours and a $2n \times 2n$ covariance matrix is formed. Principal components analysis is then used to identify the modes of greatest variability in this high-dimensional space. The ASM, thus trained, is then used to identify objects of the same class within other images. The process is initialized by identifying an orientation and scale for the mean contour and then permitting it to deform within the image in a manner analogous to that of active contours. In this case, the movement of each landmark point is to the nearest intensity gradient in a direction normal to the contour. Deformation is restricted to within the bounds of the statistical model, usually held to within three standard deviations from the mean.

The ASM has inspired enhancements, including boundary models [Duta and Sonka, 1998; van Ginneken et al., 2002], and a hierarchical formulation utilizing the wavelet transform [Davatzikos et al., 2003; Nain et al., 2007]. A shape-variant Hough transform has been used to automatically approximate the position of the object of interest in the image [Brejl and Sonka, 2000].

A level-set shape representation that does not require explicitly-defined PDMs, and that also permits surface topology modification as the model deforms, has been introduced [Leventon et al., 2000; Tsai et al., 2003]. The removal of the need for PDMs simplifies the extension of the shape model to 3D images. This approach has been further extended to permit simultaneous, coupled deformation of multiple shape models [Tsai et al., 2004].

Alternate, shape-based approaches to image segmentation have also been developed. Syntactic pattern recognition was applied to limit the deformations of snakes [Olstad and Torp, 1996]. Curve and surface representations using a set of basis functions and related parameters, where shape information is encoded in the parameters, have been used as deformable models. The shape can be changed to match an image object by allowing the parameters to evolve within statistical distributions derived from a training set. Examples include sinusoidal basis functions [Staib and Duncan, 1992; Staib and Duncan, 1996], spherical harmonics [Kelemen et al., 1999], and B-splines [Pitiot et al., 2002]. Medial (skeleton) representation of shape [Pizer et al., 2003; Yushkevich et al., 2006b] has also been used in

deformable model-based segmentation. Additionally, an approach based on information theory was used to combine pixel classification, edge detection, and shape constraints for multiple simultaneous boundary extraction in 2D CT images [Hibbard, 2004].

4.5. Appearance Models

An active appearance model (AAM) is a further development of the ASM where shape plus intensity of an object, referred to as an image patch, and corresponding variability are integrated into a statistical model [Cootes et al., 2001]. Level-set implementations of shape-plus-intensity models in 3D are described by Yang and Duncan (2004) and by Hu and Collins (2007). A brief survey describing a number of AAM variants along with a method for increasing AAM robustness is given by Beichel et al. (2005).

4.6. Deformable Organisms

Artificial organisms have also been applied to segmentation of MR images [McInerney et al., 2002]. These represent further developments of deformable models. They include a body capable of taking the shape of the desired image object and having distributed sensors and rudimentary brains with centres for perception, cognition, and motor control. They are capable of voluntary movement and alteration of body shape based on sensory input from the image and anatomical knowledge. As such, the artificial organism released into the image environment will seek out and conform to the object of interest.

5. Segmentation Software

Medical image segmentation software is available commercially from a number of sources, typically as a subset of a larger software package intended for general, interactive, image processing. Also, over the past few years, the amount of software provided without charge has grown rapidly. Supported by government, academic institutions, and individuals, this software often includes the high–level language computer program, referred to as open source.

A sampling of the available software is given in the following sections. A larger list is maintained in the Internet Analysis Tools Registry (http://www.cma.mgh.harvard.edu/iatr/) by the Center for Morphometric Analysis (CMA) at the Massachusetts General Hospital (MGH), an affiliate of Harvard University. Additionally, the Neuro Image Analysis group at the University of North Carolina at Chapel Hill maintains a webpage with links to a number of related sites where free software can be downloaded (http://www.ia.unc.edu/dev/download/). Also, free image display, analysis, and file-conversion software is available through http://www.idoimaging.com, the personal project of one radiology programmer.

5.1. BIC Software Toolbox

The McConnell Brain Imaging Centre (BIC) of the Montreal Neurological Institute (MNI) at McGill University freely offers a variety of software for medical image analysis (http://www.bic.mni.mcgill.ca/software/). Included are tools for automatic registration (ANIMAL), segmentation (INSECT), intensity nonuniformity correction (N3), sulcus extraction and labeling (SEAL), and cortex extraction. Tools for PET and fMRI analysis are also available as are a number of display and image-editing functions. A description of some of the software modules and a technique for application to the analysis of large image databases is described by Evans (2005). Demonstration videos of atlas-based software are available at http://www.bic.mni.mcgill.ca/demos/animal/.

Source code is available. All image data are stored in Medical Image NetCDF (MINC) file format. An interface to Matlab® (http://www.mathworks.com/products/matlab/) (EMMA) is also available.

5.2. BrainSuite

The BrainSuite software (http://brainsuite.usc.edu/) is produced and freely distributed as a joint project between the Laboratory of Neuro Imaging (LONI) at the University of California at Los Angeles (UCLA) (http://www.loni.ucla.edu/) and the Biomedical Imaging Research Lab of the Signal and Image Processing Institute within the Electrical Engineering department at the University of Southern California (USC) (http://neuroimage.usc.edu/). It allows skull and scalp surface extraction, cortical surface extraction, surface topology correction, and surface/image visualization. It is compatible with the BrainStorm software, also from USC, a free Matlab® toolkit for EEG and MEG data visualization and processing.

5.3. SPM

Statistical Parametric Mapping (SPM) developed at the Wellcome Department of Cognitive Neurology, University College of London, England, is freely-available software intended for analysis of brain imaging data sequences (http://www.fil.ion.ucl.ac.uk/spm/). It runs under Matlab®. Supported modalities include fMRI, PET, SPECT, EEG, and Magnetoencephalogram (MEG).

Segmentation in SPM has developed as the product has developed. The current revision, SPM5, uses the atlas-based method described by Ashburner and Friston (2005). The previous revision, SPM2, used the maximum-likelihood, statistical-clustering method described by Ashburner and Friston (1997). This segmentation algorithm has been included in a quantitative evaluation [Zaidi et al., 2006] where it was compared with the method of Van Leemput et al. (1999). Improvement in the segmentation accuracy of SPM2 has also been reported when an initial skull stripping step is performed [Fein et al., 2006].

5.4. FSL

The FMRIB Software Library (FSL) was developed by the Oxford Center for Functional Magnetic Resonance Imaging of the Brain (FMRIB) at the University of Oxford, England. The software is a library of statistical and image analysis tools for fMRI, structural MRI, and Diffusion Tensor Imaging (DTI) data [Smith et al., 2004]. The FSL software is freely available for noncommercial use (http://www.fmrib.ox.ac.uk/fsl/).

Segmentation is performed by application of an automated, brain extraction tool (BET) based on a deformable model. This is followed by automatic segmentation of gray matter, white matter, and cerebrospinal fluid using the hidden Markov random field and expectation–maximization, statistical-clustering approach of Zhang et al. (2001). The segmentation in Fig. 1(b) has been formed using this method. A method for segmentation of subcortical brain structures is also available along with a set of brain atlases. Additionally, inner skull, outer skull, and outer scalp surface representations can be obtained although this feature performs best when both T1- and T2-weighted MR images are available.

A PET partial-volume correction study employed the FSL segmentation method in comparison with the segmentation algorithm from SPM2 [Kloet et al., 2006]. Also, the BET software has been comparatively evaluated [Fennema-Notestine et al., 2006; Hartley et al., 2006].

5.5. EIKONA3D

Eikona3D (http://www.alphatecltd.com/eikona3d/imageprocessing3d.html) is a commercial software package developed by Alpha Tec, Ltd., located in Thessaloniki, Greece. The software contains a core set of image processing and visualization tools. Interactive image segmentation can be performed by threshold and by region-based methods such as region growing and region split-merge. A number of edge detection features are also available.

5.6. FreeSurfer

FreeSurfer (http://surfer.nmr.mgh.harvard.edu/) [Dale et al., 1999; Fischl et al., 1999; Fischl et al., 2001; Ségonne et al., 2004] is a software package developed by CorTechs Labs (http://www.cortechs.net/) and the Athinoula A. Martinos Center for Biomedical Imaging (http://www.nmr.mgh.harvard.edu/martinos/) at the Massachusetts General Hospital, an affiliate of Harvard University. The software employs automatic and manual segmentation methods for semiautomatic reconstruction of the cerebral cortex from structural, MR images and also allows overlay of fMRI and EEG data onto the reconstructed surface.

A quantitative evaluation of the cortical reconstruction obtained from FreeSurfer is described by Lee et al. (2006), where comparison is made with the method of Kim et al. (2005). Additionally, the technique used in FreeSurfer for removing the scalp and skull has also been compared with the BET software from FSL [Fennema-Notestine et al., 2006]. A study evaluating the surface-flattening algorithm, part of the FreeSurfer software, has also been performed [Ju et al., 2005].

5.7. Insight Segmentation and Registration Toolkit

The insight segmentation and registration toolkit (ITK) (http://www.itk.org/) and its companion the visualization toolkit (VTK) (http://public.kitware.com/VTK/) have been developed by the United States National Library of Medicine in support of the Visible Human Project. Development began in 1999 and is ongoing. The toolkits are open-source, freely available, software modules written in the C++ computer language and supported by Kitware (http://www.kitware.com/), a professional software development corporation, and also by qualified volunteers. The software modules are intended for use

in image segmentation and registration computer-software applications but are not full-fledged applications, themselves.

The segmentation modules include a variety of low-level methods such as thresholds and region growing as well as higher-level segmentation using the watershed algorithm, level-set deformable models, fuzzy connectedness, and statistical classifiers.

A stand-alone, segmentation software application called SNAP [Yushkevich et al., 2006a], for Snake Automated Partitioning, was developed using level-set algorithms in ITK and is freely distributed as open-source software (http://www.itksnap.org/). The 3D surface shown in Fig. 2 was formed using the SNAP application.

5.8. Analyze

Analyze (http://www.analyzedirect.com/Analyze) is a commercial, image analysis, software package developed by the Biomedical Imaging Resource at the Mayo Foundation based in Rochester, Minnesota, USA. Of all available software it appears to have the longest history, beginning in the early 1970's, and has impressive capabilities for volume and surface visualization, including the ability to generate cine fly-through image sequences for virtual endoscopy.

The software supports segmentation by thresholds, region growing, pixel classification, morphological operations, and interactive, manual operations. Segmentation using ITK modules is also included and a 3D brain atlas is also available.

5.9. 3D Slicer

The 3D Slicer software (http://www.slicer.org/) is developed by the MIT Artificial Intelligence Lab and the Surgical Planning Lab at Brigham and Women's Hospital, an affiliate of Harvard Medical School. It is open-source, freely-available software based on ITK and VTK. It contains functions for formation, visualization, and quantification of 3D surfaces and volumes. Segmentation is performed via a variety of methods including low-level, manual and semiautomatic tools, as well as level-sets, and atlas-based, statistical clustering using the expectation-maximization algorithm.

5.10. CAVASS

The Computer Assisted Visualization and Analysis Software System [Grevera et al., 2007] is freely available from the Medical Image Processing Group (http://mipgsun.mipg.upenn.edu/~cavass/) within the Department of Radiology at the University of Pennsylvania. It is a major revision of the 3DVIEWNIX software, previously available from the same group. It contains tools for image analysis, visualization, and object manipulation as well as interfaces to ITK, Matlab®, and CAD/CAM software packages. Its segmentation features include fuzzy connectedness [Udupa and Samarasekera, 1996] and semiautomatic edge tracing using Live Wire [Falcão et al., 1998].

5.11. MIPAV

The Medical Image Processing, Analysis, and Visualization software package is freely available from the Center for Information Technology (http://mipav.cit.nih.gov/) within the United States National Institutes of Health. It has been supported by software developed at the Laboratory for Medical Image Computing (http://medic.rad.jhmi.edu/) at Johns Hopkins University (e.g. [Bazin et al., 2007a]). The software enables quantitative analysis and visualization of medical images from a number of modalities, including MR and CT. Its segmentation functions incorporate atlas-based tissue labeling, deformable models, and fuzzy c-means clustering, including the robust, adaptive approach of Pham (2001). A number of manual and semi-automatic tools and an interface with ITK are also available.

6. Databases for Segmentation Validation

The use of automatic segmentation methods requires evaluation against a truth model to obtain a quantitative measurement of the efficacy of a given algorithm. Evaluation of results from segmentation of in vivo images is usually accomplished by comparison with segmentations made by experts. Additional evaluation of an algorithm is possible by the analysis of synthetic images or images of physical phantoms [Pham et al., 2000].

6.1. MNI

The McConnell Brain Imaging Centre of the Montreal Neurological Institute has developed a synthetic image database, called brainweb (http://www.bic.mni.mcgill.ca/brainweb/). The synthetic images were produced by passing a manually segmented head image through an MR simulator,

permitting the formation of synthetic images with specified levels of noise and intensity nonuniformity. The initial configuration contained two anatomical models, one of a normal brain and the other of a brain with multiple sclerosis lesions. The ground truth (manual) segmentation identified nine normal tissue classes and specified partial-volume content levels for each image pixel. A further twenty normal models have been recently added based on 11 normal tissue classes [Aubert-Broche et al., 2006a,b]. The image shown in Fig. 3(a) is from the MNI brainweb database.

6.2. IBSR

The Internet Brain Segmentation Repository (IBSR) (http://www.cma.mgh.harvard.edu/ibsr/) is an on-line database of MR images with manually-guided segmentations and is maintained by the Center for Morphometric Analysis (CMA) at the Massachusetts General Hospital (MGH). Head images of more than 40 subjects are available. In some images the segmentation identifies three tissue classes, gray matter, white matter, and cerebrospinal fluid (CSF). In others, up to 43 individual structures have been manually identified. IBSR images have been used in the formation of Fig. 1 and Fig. 2.

6.3. SBIA

The Section for Biomedical Image Analysis (SBIA) in the department of Radiology at the University of Pennsylvania (http://www.rad.upenn.edu/sbia/) has developed software for generating simulated inter-subject head deformations. This is intended for validation studies of atlas-based segmentation methods [Xue et al., 2006].

7. Discussion

7.1. Method Summary

Figure 4 shows a summary of all segmentation methods listed in the description of the three generations of medical image segmentation. The methods are grouped into two categories, defining the primary segmentation output, volume or boundary, for each type of method. Some methods, i.e, graph search, neural networks, multiresolution, atlas-based, and rule-based approaches, can be applied to form either category of output.

Figure 5 shows an alternate summary of the same methods organized into three categories based on the primary mode of operation: Region-based methods, boundary-following methods, and pixel-classification methods. These are the three categories that characterize the first generation. For each category, the methods corresponding to each generation are listed and the linkages between generations become visible. As with Fig. 4, some methods can be applied in more than one category. For example, the Watershed algorithm and Fuzzy Connectedness are applications of graph-search methods where the mode of operation is related to region growing, while Live Wire is an application of graph searching that operates in a mode related to that of first-generation edge tracing.

The region-based and pixel classification categories have seen intense research up to, and including, the third generation where shape models and atlas-based, statistical clustering have been of particular interest. One notable item is the relative scarcity of third-generation, boundary-following methods where only one method, that of Färber et al. (2007), has been identified. Further development in this category may be useful when it is considered that boundary following is an important part of the segmentation methodology used by medical experts.

7.2. Texture Features

For a given pixel in an image, texture features can be computed from the distribution of pixel intensity levels in a local region surrounding the pixel. Although regions of relatively uniform intensity have often been important for segmentation, other texture features have also been used to assist in the segmentation process. Texture features have been used for determining seed pixel selection and as a homogeneity criterion in region growing (e.g. Kim and Park (2004), Rivera-Rovelo and Bayro-Corrochano (2007)), and in second-generation, feature-based classification schemes including neural networks and genetic algorithms [Delibasis et al., 1997, Tsai D-Y et al., 2004]. Texture is incorporated explicitly in active appearance models [Hu and Collins, 2007], among the third generation methods, and has also been used in rule-based systems [Pitiot et al., 2004]. A history of the development of texture characterization and feature computation can be found in Arivazhagan and Ganesan (2003) along with the description of a texture segmentation system utilizing wavelet-based feature extraction.

7.3. Electrical Modelling

One of the applications where segmentation results are of particular use is in the formation of patient-specific, realistic, tissue models such as those used in EEG source analysis. The segmentation process takes a structural, medical image as input and identifies regions associated with a set of tissue classes. Given conductance values for each such class, an electrical conductivity model, specific to the individual represented in the image, can be produced from the segmentation data. It has been shown that the use of realistic, electrical, head models produces improvements in the accuracy of EEG source-localization techniques [Roth et al., 1993; Cuffin, 1996; Huiskamp et al., 1999].

While the emergence of new technologies such as diffusion tensor imaging (DTI) [Tuch et al., 2001], electrical impedance tomography (EIT) [Goncalves et al., 2003] and others [Gutierrez et al., 2004] might one day lessen the importance of segmentation in head modeling, it is not likely that this supplantation will be complete any time soon. DTI, on one hand, provides exquisite images of the diffusivity of water molecules in gray and white matter in the brain that can be used to estimate tissue conductivity, but its utility for providing this information for skull tissue is very poor. On the other hand, while the utility of EIT for measuring the conductivity of skull tissue is good, the spatial resolution provided by this technology leaves much to be desired. Automatic and precise segmentation of head images for EEG source analysis will remain an important tool for at least the head, skull and brain boundaries and also for the gray matter - white matter interface. This interface is critical for accurately defining the solution space required for estimating the source activity in the cerebral cortex underlying the EEG.

7.4. Segmentation Development

The goal of automatic medical image segmentation research is that of a fully–automatic, unsupervised solution with accuracy matching a human medical expert. It is clear that first-generation methods were not successful and it becomes more and more evident that second-generation methods, despite obvious improvements and mathematical superiority, will likewise prove to be insufficient. The second generation has produced fully-automatic segmentation systems; however, obvious misclassification may still occur. The application of optimization methods alone cannot guarantee that segmentation results will be anatomically meaningful, and results are, therefore, strongly data dependent. Segmentation output from all second-generation methods can be expected to require manual correction to be clinically useful.

Among the third-generation algorithms, certain atlas-based methods have been shown to produce automatic segmentations that are competitive with manual segmentations when an overlap metric (e.g. the ratio of the intersection of two segmentations to their union) is used for the comparison [Fischl et al., 2002; Zijdenbos et al., 2002; Carmichael et al., 2005]. There is indication, though, that such favourable comparison may only occur under certain conditions [Carmichael et al., 2005]. Factors that can affect algorithm performance include: 1) the image acquisition parameters; 2) the method for registering the atlas with the test image where registration methods capable of greater deformation produce better comparison results; 3) the manual tracing protocol used by the investigator, which, when identifying normal brain structures, must match that used in the atlas formation for best comparison; and, 4) demographics and disease where differences in brain structure between the test subjects and the subjects included in atlas formation may cause significant errors. In addition, the overlap metric may not adequately identify errors in cases where discrepancies between the two segmentations under examination have relatively small volume. These errors could still be spatially significant, for example, in the case of a narrow projection occurring in only one of the segmentations.

8. Conclusion

The three generations of medical image segmentation show the dramatic growth in algorithmic capability over the past 35 years and provide a mechanism for classifying the many methods that have been devised. Continued development of medical image segmentation methods can be expected until the goal of accurate, fully-automatic, unsupervised segmentation has been achieved.
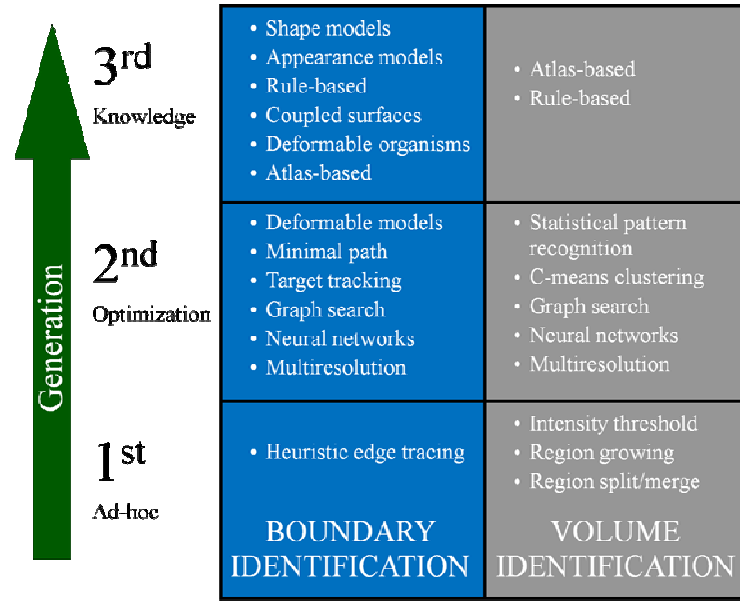
Figure 4. *Method summary with categories based on primary segmentation output.*
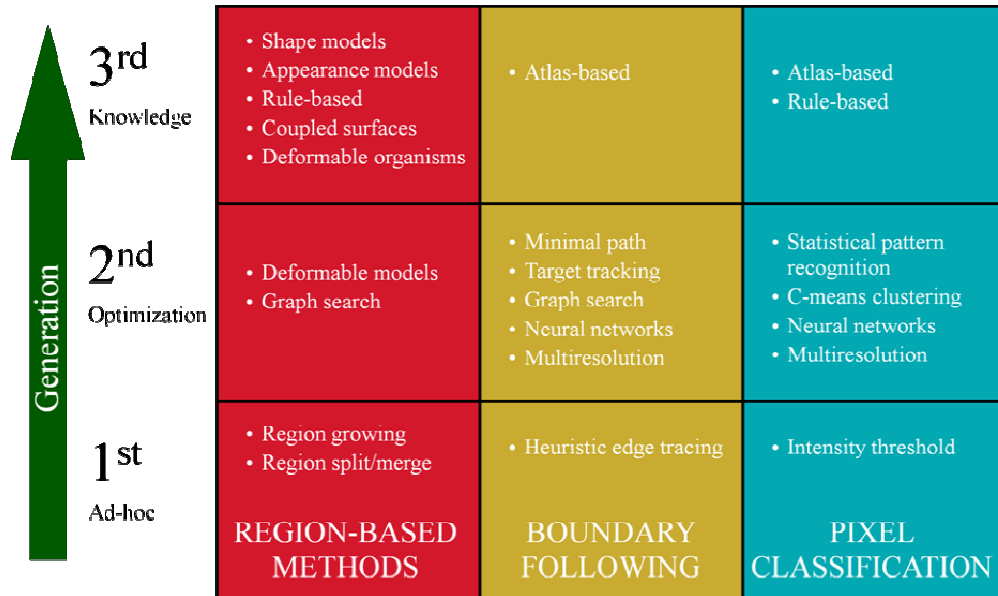

Figure 5. *Method summary with categories based on mode of operation.*

References

Abolmaesumi P, Sirouspour MR. An interacting multiple model probabilistic data association filter for cavity boundary extraction from ultrasound images. *IEEE Transactions on Medical Imaging*, 23(6): 772-784, 2004.

Ahmed MN, Yamany SM, Mohamed N, Farag AA, Moriarty T. A modified fuzzy c-means algorithm for bias field estimation and segmentation of MRI data. *IEEE Transactions on Medical Imaging*, 21(3): 193-199, 2002.

Algorri M-E, Flores-Mangas F. Classification of anatomical structures in MR brain images using fuzzy parameters. *IEEE Transactions on Biomedical Engineering*, 51(9): 1599-1608, 2004.

Amato U, Larobina M, Antoniadis A, Alfano B. Segmentation of magnetic resonance brain images through discriminant analysis. *Journal of Neuroscience Methods*, 131: 65-74, 2003.

Amini L, Soltanian-Zadeh H, Lucas C, Gity M. Automatic segmentation of thalamus from brain MRI integrating fuzzy clustering and dynamic contours. *IEEE Transactions on Biomedical Engineering*, 51(5): 800-811, 2004.

Anbeek P, Vincken KL, van Bochove GS, van Osch MJP, van der Grond J. Probabilistic segmentation of brain tissue in MR imaging. *NeuroImage*, 27: 795-804, 2005.

Angenent S, Pichon E, Tannenbaum A. Mathematical methods in medical image processing. *Bulletin (New Series) of the American Mathematical Society*, 43(3): 365-396, 2006.

Appleton B, Talbot H. Globally minimal surfaces by continuous maximal flows. *IEEE Transactions on Pattern Analysis and Machine Intelligence*, 28(1): 106-118, 2006.

Arata LK, Dhawan AP, Broderick JP, Gaskil-Shipley MF, Levy AV, Volkow ND. Three-dimensional anatomical model-based segmentation of MR brain images through principal axes registration. *IEEE Transactions on Biomedical Engineering*, 42(11): 1069-1078, 1995.

Ardon R, Cohen LD, Yezzi A. A new implicit method for surface segmentation by minimal paths in 3D images. *Applied Mathematics and Optimization*, 55:127-144, 2007.

Arivazhagan S, Ganesan L. Texture segmentation using wavelet transform. *Pattern Recognition Letters*, 24: 3197-3203, 2003.

Ashburner J, Friston K. Multimodal image coregistrations and partitioning – A unified framework. *NeuroImage*, 6(3): 209-217, 1997.

Ashburner J, Friston KJ. Unified segmentation. *NeuroImage*, 26: 839-851, 2005.

Ashton EA, Berg MJ, Parker KJ, Weisberg J, Chen CW, Ketonen L. Segmentation and feature extraction techniques with applications to MRI head studies. *Magnetic Resonance in Medicine*, 33: 670-677, 1995.

Aubert-Broche B, Evans AC, Collins L. A new improved version of the realistic digital brain phantom. *NeuroImage*, 32: 138-145, 2006a.

Aubert-Broche B, Griffin M, Pike GB, Evans AC, Collins DL. Twenty new digital brain phantoms for creation of validation image data bases. *IEEE Transactions on Medical Imaging*, 25(11): 1410-1416, 2006b.

Barra V, Boire J-Y. Automatic segmentation of subcortical brain structures in MR images using information fusion. *IEEE Transactions on Medical Imaging*, 20(7): 549-558, 2001.

Barrett WA, Mortensen EN. Interactive live wire boundary extraction. *Medical Image Analysis*, 1(4): 331-341, 1997.

Barrios V, Torres J, Montilla G, Hernandez L, Rangel N, Reigosa A. Cellular edge detection using a trained neural network explorer. In proceedings of the 16th Annual International Conference IEEE Engineering in Medicine and Biology Society, Vol. 2, 1994, 1075-1076.

Bazin P-L, Cuzzocreo JL, Yassa MA, Gandler W, McAuliffe MJ, Bassett SS, Pham DL. Volumetric neuroimage analysis extensions for the MIPAV software package. *Journal of Neuroscience Methods*, 165: 111-121, 2007a.

Bazin P-L, Pham DL. Topology-preserving tissue classification of magnetic resonance brain images. *IEEE Transactions on Medical Imaging*, 26(4): 487-496, 2007b.

Beichel R, Bischof H, Leberl F, Sonka M. Robust active appearance models and their application to medical image analysis. *IEEE Transactions on Medical Imaging*, 24(9): 1151-1169, 2005.

Bezdek JC, Hall LO, Clarke LP. Review of MR image segmentation techniques using pattern recognition. *Medical Physics,* 20(4): 1033-1048, 1993.

Bezdek JC, Hall LO, Clark MC, Goldgof DB, Clarke LP. Medical image analysis with fuzzy models. *Statistical Methods in Medical Research*, 6: 191-214, 1997.

Boskovitz V, Guterman H. An adaptive neuro-fuzzy system for automatic image segmentation and edge detection. *IEEE Transactions on Fuzzy Systems*, 10(2): 247-262, 2002.

Bouix S, Martin-Fernandez M, Ungar L, Nakamura M, Koo M-S, McCarley RW, Shenton ME. On evaluating brain tissue classifiers without a ground truth. *NeuroImage*, 36: 1207-1224, 2007.

Boykov Y, Funka-Lea G. Graph cuts and efficient N-D image segmentation. *International Journal of Computer Vision*, 70(2): 109-131, 2006.

Brejl M, Sonka M. Object localization and border detection criteria design in edge-based image segmentation: Automated learning from examples. *IEEE Transactions on Medical Imaging*, 19(10): 973-985, 2000.

Bresson X, Esedoglu S, Vandergheynst P, Thiran J-P, Osher S. Fast global minimization of the active contour/snake model. *Journal of Mathematical Imaging and Vision*, 28: 151-167, 2007.

Cappelletti JD, Rosenfeld A. Three-dimensional boundary following. *Computer Vision, Graphics, and Image Processing*, 48: 80-92, 1989.

Carmichael OT, Aizenstein HA, Davis SW, Becker JT, Thompson PM, Meltzer CC, Liu Y. Atlas-based hippocampus segmentation in Alzheimer's disease and mild cognitive impairment. *NeuroImage*, 27: 979-990, 2005.

Caselles V, Kimmel R, Sapiro G. Geodesic active contours. *International Journal of Computer Vision*, 22(1): 61-79, 1997a.

Caselles V, Kimmel R, Sapiro G, Sbert C. Minimal surfaces based object segmentation. *IEEE Transactions on Pattern Analysis and Machine Intelligence*, 19(4): 394-398, 1997b.

Chakraborty A, Staib LH, Duncan JS. Deformable boundary finding in medical images by integrating gradient and region information. *IEEE Transactions on Medical Imaging*, 15(6): 859-870, 1996.

Chan TF, Vese LA. Active contours without edges. *IEEE Transactions on Image Processing*, 10(2): 266-277, 2001.

Chellappa R, Jain A, eds. Markov Random Fields Theory and Application. Academic Press, 1993.

Chen CW, Luo J, Parker KJ. Image segmentation via adaptive K-mean clustering and knowledge-based morphological operations with biomedical applications. *IEEE Transactions on Image Processing*, 7(12): 1673-1683, 1998.

Chung DH, Sapiro G. Segmenting skin lesions with partial-differential-equations-based image processing algorithms. *IEEE Transactions on Medical Imaging*, 19(7): 763-767, 2000.

Clark MC, Hall LO, Goldgof DB, Velthuizen R, Murtagh FR, Silbiger MS. Automatic tumor segmentation using knowledge-based techniques. *IEEE Transactions on Medical Imaging*, 17(2): 187-201, 1998.

Clarke LP, Velthuizen RP, Phuphanich S, Schellenberg JD, Arrington JA, Silbiger M. MRI: Stability of three supervised segmentation techniques. *Magnetic Resonance Imaging*, 11(1): 95-106, 1993.

Clarke LP, Velthuizen RP, Camacho MA, Heine JJ, Vaidyanathan M, Hall LO, Thatcher RW, Silbiger ML. MRI segmentation: Methods and applications. *Magnetic Resonance Imaging*, 13(3): 343-368, 1995.

Cocosco CA, Zijdenbos AP, Evans AC. A fully automatic and robust brain MRI tissue classification method. *Medical Image Analysis*, 7: 513-527, 2003.

Cohen LD, Kimmel R. Global minimum for active contour models: A minimal path approach. *International Journal of Computer Vision*, 24(1): 57-78, 1997.

Collins DL, Holmes CJ, Peters TM, Evans AC. Automatic 3-D model-based neuroanatomical segmentation. *Human Brain Mapping*, 3(3): 190-208, 1995.

Cootes TF, Taylor CJ, Cooper DH, Graham J. Active shape models – Their training and application. *Computer Vision and Image Understanding*, 61(1): 38-59, 1995.

Cootes TF, Edwards GJ, Taylor CJ. Active appearance models. *IEEE Transactions on Pattern Analysis and Machine Intelligence*, 23(6): 681-685, 2001.

Cuffin BN. EEG localization accuracy improvements using realistically shaped head models. *IEEE Transactions on Biomedical Engineering*, 43(3): 299-303, 1996.

Dade LA, Gao FQ, Kovacevic N, Roy P, Rockel C, O'Toole CM, Lobaugh NJ, Feinstein A, Levine B, Black SE. Semiautomatic brain region extraction: A method of parcellating brain regions from structural magnetic resonance images. *NeuroImage*, 22: 1492-1502, 2004.

Dale AM, Fischl B, Sereno MI. Cortical surface-based analysis I: Segmentation and surface reconstruction. *NeuroImage*, 9: 179-194, 1999.

Davatzikos C, Tao X, Shen D, "Hierarchical active shape models, using the wavelet transform," *IEEE Transactions on Medical Imaging*, 22(3): 414-423, 2003.

Dawant BM, Hartmann SL, Thirion J-P, Maes F, Vandermeulen D, Demaerel P. Automatic 3-D segmentation of internal structures of the head in MR images using a combination of similarity and free-form transformations: Part I, Methodology and validation on normal subjects. *IEEE Transactions on Medical Imaging*, 18(10): 909-916, 1999.

Delibasis K, Undrill PE, Cameron GG. Designing texture filters with genetic algorithms: An application to medical images. *Signal Processing*, 57: 19-33, 1997.

Duncan JS, Ayache N. Medical image analysis: Progress over two decades and the challenges ahead. *IEEE Transactions on Pattern Analysis and Machine Intelligence*, 22(1): 85-106, 2000.

Duta N, Sonka M. Segmentation and interpretation of MR brain images: An improved active shape model. *IEEE Transactions on Medical Imaging*, 17(6): 1049-1062, 1998.

Eckhorn R. Neural mechanisms of scene segmentation: Recordings from the visual cortex suggest basic circuits for linking field models. *IEEE Transactions on Neural Networks*, 10(3): 464-479, 1999.

Ehricke H-H. Automated 3D MR image analysis with a rule-based segmentation system. In proceedings of CAR '91, Computer Assisted Radiology, Berlin, Germany: Springer Verlag, 1991, 543-548.

Evans AC. Large-scale morphometric analysis of neuroanatomy and neuropathology. *Anatomy and Embryology*, 210: 439-446, 2005.

Falcão AX, Udupa JK, Samarasekera S, Sharma S. User-steered image segmentation paradigms: Live wire and live lane. *Graphical Models and Image Processing,* 60: 233-260, 1998.

Falcão AX, Udupa JK. A 3D generalization of user-steered live-wire segmentation. *Medical Image Analysis*, 4: 389-402, 2000.

Falcão AX, Udupa JK, Miyazawa FK. An ultra-fast user-steered image segmentation paradigm: Live wire on the fly. *IEEE Transactions on Medical Imaging,* 19(1): 55-62, 2000.

Falcão AX, Stolfi J, de Alencar Lotufo R. The image foresting transform: Theory, algorithms, and applications. *IEEE transactions on Pattern Analysis and Machine Intelligence*, 26(1): 19-29, 2004.

Färber M, Erhardt J, Handels H. Live-wire-based segmentation using similarities between corresponding image structures. *Computerized Medical Imaging and Graphics*, 31: 549-560, 2007.

Fein G, Landman B, Tran H, Barakos J, Moon K, Di Sclafani V, Schumway R. Statistical parametric mapping of brain morphology: Sensitivity is dramatically increased by using brain-extracted images as inputs. *NeuroImage*, 30: 1187-1195, 2006.

Fennema-Notestine C, Ozyurt IB, Clark CP, Morris S, Bischoff-Grethe A, Bondi MW, Jernigan TL, Fischl B, Segonne F, Shattuck DW, Leahy RM, Rex DE, Toga AW, Zou KH, Birn M, Brown GG. Quantitative evaluation of automated skull-stripping methods applied to contemporary and legacy images: Effects of diagnosis, bias correction, and slice location. *Human Brain Mapping*, 27: 99-113, 2006.

Fischl B, Sereno MI, Dale AM. Cortical surface-based analysis II:. Inflation, flattening, and a surface-based coordinate system. *NeuroImage*, 9: 195-207, 1999.

Fischl B, Liu A, Dale AM. Automated manifold surgery: Constructing geometrically accurate and topologically correct models of the human cerebral cortex. *IEEE Transactions on Medical Imaging*, 20(1): 70-80, 2001.

Fischl B, Salat DH, Busa E, Albert M, Dieterich M, Haselgrove C, van der Kouwe A, Killiany R, Kennedy D, Klaveness S, Montillo A, Makris N, Rosen B, Dale AM. Whole brain segmentation: Automated labeling of neuroanatomical structures in the human brain. *Neuron*, 33: 341-355, 2002.

Fischl B, Salat DH, van der Kouwe AJW, Makris N, Ségonne F, Quinn BT, Dale AM. Source-independent segmentation of magnetic resonance images. *NeuroImage*, 23: S69-S84, 2004.

Gelas A, Bernard O, Friboulet D, Prost R. Compactly supported radial basis functions based collocation method for level-set evolution in image segmentation. *IEEE Transactions on Image Processing*, 16(7): 1873-1886, 2007.

González Ballester MÁ, Zisserman AP, Brady M. Estimation of the partial volume effect in MRI. *Medical Image Analysis*, 6: 389-405, 2002.

Goncalves SI, deMunck JC, Verbunt JPA, Bijma F, Heethaar RM, Lopes da Silva F. In vivo measurement of the brain and skull resistivities using an EIT-based method and realistic models for the head. *IEEE Transactions on Biomedical Engineering*, 50: 754-767, 2003.

Grevera G, Udupa J, Odhner D, Zhuge Y, Souza A, Iwanaga T, Mishra S. CAVASS: A computer-assisted visualization and analysis software system. *Journal of Digital Imaging*, 20(Suppl 1): 101-118, 2007.

Gutierrez D, Nehorai A, Muravchik CH. Estimating brain conductivities and dipole source signals with EEG arrays. *IEEE Transactions on Biomedical Engineering*, 51: 2113-2122, 2004.

Haacke EM, Liang Z-P. Challenges of imaging structure and function with MRI. *IEEE Engineering in Medicine and Biology*, September/October: 55-62, 2000.

Han X, Xu C, Prince JL. A topology preserving level set method for geometric deformable models. *IEEE transactions on Pattern Analysis and Machine Intelligence*, 25(6): 755-768, 2003.

Hartley SW, Schur AI, Korf ESC, White LR, Launer LJ. Analysis and validation of automated skull stripping tools: A validation study based on 296 MR images from the Honolulu Asia aging study. *NeuroImage*, 30: 1179-1186, 2006.

Hata N, Muragaki Y, Inomata T, Maruyama T, Iseki H, Hori T, Dohi T. Intraoperative tumor segmentation and volume measurement in MRI-guided glioma surgery for tumor resection rate control. *Academic Radiology,* 12(1): 116-122, 2005.

Heckemann RA, Hajnal JV, Aljabar P, Rueckert D, Hammers A. Automatic anatomical brain MRI segmentation combining label propagation and decision fusion. *NeuroImage*, 33: 115-126, 2006.

Held K, Rota Kops E, Krause BJ, Wells III WM, Kikinis R, Müller-Gärtner H-W. Markov random field segmentation of brain MR images. *IEEE Transactions on Medical Imaging*, 16(6): 878-886, 1997.

Hibbard LS. Region segmentation using information divergence measures. *Medical Image Analysis*, 8: 233-244, 2004.

Hojjatoleslami SA, Kittler J. Region growing: A new approach. *IEEE Transactions on Image Processing*, 7(7): 1079-1084, 1998.

Hojjatoleslami SA, Kruggel F. Segmentation of large brain lesions. *IEEE Transactions on Medical Imaging*, 20(7): 666-669, 2001.

Hu S, Collins DL. Joint level-set shape modeling and appearance modeling for brain structure segmentation. *NeuroImage* 36: 672-683, 2007.

Huiskamp G, Vroeijenstijn M, van Dijk R, Wieneke G, van Huffelen AC. The need for correct realistic geometry in the inverse EEG problem. *IEEE Transactions on Biomedical Engineering*, 46(11): 1281-1287, 1999.

Jain AK, Zhong Y, Dubuisson-Jolly M-P. Deformable template models: A review. *Signal Processing*, 71: 109-129, 1998.

Jain AK, Duin RPW, Mao J. Statistical pattern recognition: A review. *IEEE Transactions on Pattern Analysis and Machine Intelligence*, 22(1): 4-37, 2000.

Jiménez-Alaniz JR, Medina-Bañuelos V, Yáñez-Suárez O. Data-driven brain MRI segmentation supported on edge confidence and a priori tissue information. *IEEE Transactions on Medical Imaging*, 25(1): 74-83, 2006.

Johnson JL, Padgett ML. PCNN models and applications. *IEEE Transactions on Neural Networks*, 10(3): 480-498, 1999.

Ju L, Hurdal MK, Stern J, Rehm K, Schaper K, Rottenberg D. Quantitave evaluation of three cortical surface flattening methods. *NeuroImage*, 28: 869-880, 2005.

Kapur T, Grimson WEL, Wells III WM, Kikinis R. Segmentation of brain tissue from magnetic resonance images. *Medical Image Analysis*, 1(2): 109-127, 1996.

Kass M, Witkin A, Terzopoulos D. Snakes: Active contour models. *International Journal of Computer Vision*, 1(4): 321-331, 1988.

Kelemen A, Székely G, Gerig G. Elastic model-based segmentation of 3-D neuroradiological data sets. *IEEE Transactions on Medical Imaging*, 18(10): 828-839, 1999.

Kim D-Y, Park J-W. Computer-aided detection of kidney tumor on abdominal computed tomography scans. *Acta Radiologica*, 45: 791-795, 2004.

Kim JS, Singh V, Lee JK, Lerch J, Ad-Dab'bagh Y, MacDonald D, Lee JM, Kim SI, Evans AC. Automated 3-D extraction and evaluation of the inner and outer cortical surfaces using a Laplacian map and partial volume effect classification. *NeuroImage*, 27: 210-221, 2005.

Kloet RW, van Berckel BNM, Pouwels PJW, Schuitemaker A, Barkhof F, Kropholler MA, Lammertsma AA, Boellaard R. Effects of MR scanner type, scanning sequence, and segmentation algorithm on MR-based partial volume corrections of [^{11}C](R)-PK11195 studies. *NeuroImage*, 31: T83-T83, 2006.

Lee JK, Lee J-M, Kim JS, Kim IY, Evans AC, Kim SI. A novel quantitative cross-validation of different cortical surface reconstruction algorithms using MRI phantom. *NeuroImage*, 31: 572-584, 2006.

Letteboer MMJ, Olsen OF, Dam EB, Willems PWA, Viergever MA, Niessen WJ. Segmentation of tumors in magnetic resonance brain images using an interactive multiscale watershed algorithm. *Academic Radiology*, 11: 1125-1138, 2004.

Leventon ME, Grimson WEL, Faugeras O. Statistical shape influence in geodesic active contours. In proceedings of the IEEE Conference on Computer Vision and Pattern Recognition, Vol. 1, 2000, 316-323.

Li B, Acton ST. Active contour external force using vector field convolution for image segmentation. *IEEE Transactions on Image Processing*, 16(8): 2096-2106, 2007.

Li H, Deklerck R, De Cuyper B, Hermanus A, Nyssen E, Cornelis J. Object recognition in brain CT-scans: Knowledge-based fusion of data from multiple feature extractors. *IEEE Transactions on Medical Imaging*, 14(2): 212-229, 1995.

Li K, Wu X, Chen DZ, Sonka M. Optimal surface segmentation in volumetric images – A graph theoretic approach. *IEEE transactions on Pattern Analysis and Machine Intelligence*, 28(1): 119-134, 2006.

Liang J, McInerney T, Terzopoulos D. United snakes. *Medical Image Analysis*, 10: 215-233, 2006.

Liew AW-C, Yan H. An adaptive spatial fuzzy clustering algorithm for 3-D MR image segmentation. *IEEE Transactions on Medical Imaging*, 22(9): 1063-1075, 2003.

Lineberry M. Image segmentation by edge tracing. In proceedings of the SPIE, The International Society for Optical Engineering, Vol. 359, *Applications of Digital Image Processing 4*, San Diego, Calif., USA, 1982, 361-368.

Magnotta VA, Heckel D, Andreasen AC, Cizadlo T, Corson PW, Ehrhardt JC, Yuh WTC. Measurement of brain structures with artificial neural networks: Two- and three-dimensional applications. *Radiology*, 211:781-790, 1999.

Malladi R, Sethian JA, Vemuri BC. Shape modeling with front propagation: A level set approach. *IEEE Transactions on Pattern Analysis and Machine Intelligence*, 17(2): 158-175, 1995.

Marroquin JL, Vemuri BC, Botello S, Calderon F, Fernandez-Bouzas A. An accurate and efficient Bayesian method for automatic segmentation of brain MRI. *IEEE Transactions on Medical Imaging*, 21(8): 934-945, 2002.

Marroquin JL, Santana EA, Botello S. Hidden Markov measure field models for image segmentation. *IEEE Transactions on Pattern Analysis and Machine Intelligence*, 25(11): 1380-1387, 2003.

Martelli A. An application of heuristic search methods to edge and contour detection. *Communications of the ACM*, 19(2): 73-83, 1976.

Mazzara GP, Velthuizen RP, Pearlman JL, Greenberg HM, Wagner H. Brain tumor target volume determination for radiation treatment planning through automated MRI segmentation. *International Journal of Radiation Oncology Biology Physics*, 59(1): 300-312, 2004.

McInerney T and Terzopoulos D. Deformable models in medical image analysis: A survey. *Medical Image Analysis*, 1(2): 91-108, 1996.

McInerney T, Terzopoulos D. Topology adaptive deformable surfaces for medical image volume segmentation. *IEEE Transactions on Medical Imaging*, 18(10): 840-850, 1999.

McInerney T, Hamarneh G, Shenton M, Terzopoulos D. Deformable organisms for automatic medical image analysis. *Medical Image Analysis*, 6: 251-266, 2002.

Meegama RGN, Rajapakse JC. NURBS snakes. *Image Vision and Computing*, 21: 551-562, 2003.

M'hiri S, Cammoun L, Ghorbel F. Speeding up HMRF_EM algorithms for fast unsupervised image segmentation by bootstrap resampling: Application to the brain tissue segmentation. *Signal Processing*, 87: 2544-2559, 2007.

Michel CM, Murray MM, Lantz G, Gonzalez S, Spinelli L, Grave de Peralta R. EEG source imaging. *Clinical Neurophysiology*, 115: 2195-2222, 2004.

Middleton I, Damper RI. Segmentation of magnetic resonance images using a combination of neural networks and active contour models. *Medical Engineering and Physics*, 26: 71-86, 2004.

Montagnat J, Delingette H, Ayache N. A review of deformable surfaces: Topology, geometry, and deformation. *Image and Vision Computing*, 19: 1023-1040, 2001.

Mumford D, Shah J, "Optimal approximations by piecewise smooth functions and associated variational problems," *Communications on Pure and Applied Mathematics*, 42(5): 577-685, 1989.

Nain D, Haker S, Bobick A, Tannenbaum A. Multiscale 3-D shape representation and segmentation using spherical wavelets. *IEEE Transactions on Medical Imaging*, 26(4): 598-618, 2007.

Natarajan K, Cawley MG, Newell JA. A knowledge-based system paradigm for automatic interpretation of CT scans. *Medical Informatics*, 16(2): 167-181, 1991.

Neissen WJ, Vinken KL, Weickert J, Ter Haar Romeny BM, Viergever MA. Multiscale segmentation of three-dimensional MR brain images. *International Journal of Computer Vision*, 31: 185-202, 1999.

Ng S-K, McLachlan GJ. Speeding up the EM algorithm for mixture model-based segmentation of magnetic resonance images. *Pattern Recognition*, 37: 1573-1589, 2004.

Nikolaidis N, Pitas I. 3-D Image Processing Algorithms. John Wiley & Sons, Inc., 2001.

Olabarriaga SD, Smeulders AWM. Interaction in the segmentation of medical images: A survey. *Medical Image Analysis*, 5: 127-142, 2001.

Olstad B, Torp AH. Encoding of a priori information in active contour models. *IEEE Transactions on Pattern Analysis and Machine Intelligence*, 18(9): 863-872, 1996.

Pham DL, Prince JL. Adaptive fuzzy segmentation of magnetic resonance images. *IEEE Transactions on Medical Imaging*, 18(9): 737-752, 1999.

Pham DL, Xu C, Prince JL. Current methods in medical image segmentation. *Annual Review of Biomedical Engineering*, 2: 315-337, 2000.

Pham DL. Robust fuzzy segmentation of magnetic resonance images. In proceedings of the 14th IEEE Symposium on Computer-Based Medical Systems (CBMS2001), 2001, 127-131.

Pitas I. Digital Image Processing Algorithms. Prentice-Hall, 1993.

Pitiot A, Toga AW, Thompson PM. Adaptive elastic segmentation of brain MRI via shape-model-guided evolutionary programming. *IEEE Transactions on Medical Imaging*, 21(8): 910-923, 2002.

Pitiot A, Delingette H, Thompson PM, Ayache N. Expert knowledge-guided segmentation system for brain MRI. *NeuroImage*, 23: S85-S96, 2004.

Pizer SM, Fletcher PT, Joshi S, Thall A, Chen JZ, Fridman Y, Fritsch DS, Gash AG, Glotzer JM, Jiroutek MR, Lu C, Muller KE, Tracton G, Yushkevich P, Chaney EL. Deformable m-reps for 3D medical image segmentation. *International Journal of Computer Vision,* 55(2): 85-106, 2003.

Pohl KM, Fisher J, Grimson WEL, Kikinis R, Wells WM. A Bayesian model for joint segmentation and registration. *NeuroImage*, 31: 228-239, 2006.

Powell S, Magnotta VA, Johnson H, Jammalamadaka VK, Pierson R, Andreason NC. Registration and machine learning-based automated segmentation of subcortical and cerebellar brain structures. *NeuroImage*, 39: 238-247, 2008.

Pratt WK. Digital Image Processing. John Wiley & Sons, Inc., 1991.

Qu X, Li X. A 3D surface tracking algorithm. *Computer Vision and Image Understanding*, 64(1): 147-156, 1996.

Raff U, Newman FD. Automated lesion detection and lesion quantitation in MR images using autoassociative memory. *Medical Physics*, 19(1): 71-77, 1992.

Raman SV, Sarkar S, Boyer KL. Tissue boundary refinement in magnetic resonance images using contour-based scale space matching. *IEEE Transactions on Medical Imaging*, 10(2): 109-121, 1991.

Raya SP. Low-level segmentation of 3-D magnetic resonance brain images – A rule-based system. *IEEE Transactions on Medical Imaging*, 9(3): 327-337, 1990.

Rivera-Rovelo J, Bayro-Corrochano E. Medical image segmentation, volume representation and registration using spheres in the geometric algebra framework. *Pattern Recognition*, 40: 171-188, 2007.

Rosenfeld A. On connectivity properties of grayscale pictures. *Pattern Recognition,* 16(1): 47-50, 1983.

Rosenfeld A. The fuzzy geometry of image subsets. *Pattern Recognition Letters*, 2: 311-317, 1984.

Roth BJ, Balish M, Gorbach A, Sato S. How well does a three-sphere model predict positions of dipoles in a realistically shaped head? *Electroencephalography and Clinical Neurophysiology*, 87: 175-184, 1993.

Ségonne F, Dale AM, Busa E, Glessner M, Salat D, Hahn HK, Fischl B. A hybrid approach to the skull stripping problem in MRI. *NeuroImage*, 22: 1060-1075, 2004.

Sethian JA. Level set methods and fast marching methods. Cambridge University Press, 1999.

Shareef N, Wang DL, Yagel R. Segmentation of medical images using LEGION. *IEEE Transactions on Medical Imaging*, 18(1): 74-91, 1999.

Shattuck DW, Mirza M, Adisetiyo V, Hojatkashani C, Salamon G, Narr KL, Poldrack RA, Bilder RM, Toga AW. Construction of a 3D probabilistic atlas of human cortical structures. *NeuroImage*, 39: 1064-1080, 2008.

Smith SM, Jenkinson M, Woolrich MW, Beckmann CF, Behrens TEJ, Johansen-Berg H, Bannister PR, De Luca M, Drobnjak I, Flitney DE, Niazy RK, Saunders J, Vickers J, Zhang Y, De Stefano N, Brady JM, Matthews PM. Advances in functional and structural MR image analysis and implementation as FSL. *NeuroImage*, 23: S208-S219, 2004.

Solaiman B, Debon R, Pipelier F, Cauvin J-M, Roux C. Information fusion: Application to data and model fusion for ultrasound image segmentation. *IEEE Transactions on Biomedical Engineering*, 46(10): 1171-1175, 1999.

Soltanian-Zadeh H, Windham JP. A multiresolution approach for contour extraction from brain images. *Medical Physics*, 24(12): 1844-1853, 1997.

Sonka M, Tadikonda SK, Collins SM. Knowledge-based interpretation of MR brain images. *IEEE Transactions on Medical Imaging*, 15(4): 443-452, 1996.

Staib LH, Duncan JS. Boundary finding with parametrically deformable models. *IEEE Transactions on Pattern Analysis and Machine Intelligence*, 14(11): 1061-1075, 1992.

Staib LH, Duncan JS. Model-based deformable surface finding for medical images. *IEEE Transactions on Medical Imaging*, 15(5): 720-731, 1996.

Sum KW, Cheung PYS. Boundary vector field for parametric active contours. *Pattern Recognition*, 40: 1635-1645, 2007.

Suri JS, Singh S, Reden L. Computer vision and pattern recognition techniques for 2-D and 3-D MR cerebral cortical segmentation (Part 1): A state-of-the-art review. *Pattern Analysis and Applications*, 5: 46-76, 2002a.

Suri JS, Singh S, Reden L. Fusion of region and boundary/surface-based computer vision and pattern recognition techniques for 2-D and 3-D MR cerebral cortical segmentation (Part 2): A state-of-the-art review. *Pattern Analysis and Applications*, 5: 77-98, 2002b.

Suzuki H, Toriwaki J. Automatic segmentation of head MRI images by knowledge guided thresholding. *Computerized Medical Imaging and Graphics*, 15(4): 233-240, 1991.

Tohka J, Zijdenbos A, Evans AC. Fast and robust parameter estimation for statistical partial volume models in brain MRI. *NeuroImage*, 23: 84-97, 2004.

Tsai A, Yezzi Jr A, Willsky AS. Curve evolution implementation of the Mumford-Shah functional for image segmentation, denoising, interpolation, and magnification. *IEEE Transactions on Image Processing*, 10(8): 1169-1186, 2001.

Tsai A, Yezzi Jr A, Wells W, Tempany C, Tucker D, Fan A, Grimson WE, Willsky A. A shape-based approach to the segmentation of medical imagery using level sets. *IEEE Transactions on Medical Imaging*, 22(2): 137-154, 2003.

Tsai A, Wells W, Tempany C, Grimson E, Willsky A. Mutual information in coupled multi-shape model for medical image segmentation. *Medical Image Analysis*, 8: 429-445, 2004.

Tsai D-Y, Lee Y, Sekiya M, Ohkubo M. Medical image classification using genetic-algorithm based fuzzy-logic approach. *Journal of Electronic Imaging*, 13(4): 780-788, 2004.

Tuch DS, Wedeen VJ, Dale AM, George JS, Belliveau JW. Conductivity tensor mapping of the human brain using diffusion tensor MRI. *Proceedings of the National Academy of Sciences of the United States of America*, 98: 11697-11701, 2001.

Udupa JK, Samarasekera S. Fuzzy connectedness and object definition: Theory, algorithms, and applications in image segmentation. *Graphical Models and Image Processing*, 58(3): 246-261, 1996.

Udupa JK, Saha PK. Fuzzy connectedness and image segmentation. *Proceedings of the IEEE,* 91(10): 1649-1669, 2003.

van Ginneken B, Frangi AF, Staal JJ, ter Haar Romeny BM, Viergever MA. Active shape model segmentation with optimal features. *IEEE Transactions on Medical Imaging*, 21(8): 924-933, 2002.

Van Leemput K, Maes F, Vandermeulen D, Suetens P. Automated model-based tissue classification of MR images of the brain. *IEEE Transactions on Medical Imaging*, 18(10): 897-908, 1999.

Van Leemput K, Maes F, Vandermeulen D, Suetens P. A unifying framework for partial volume segmentation of brain MR images. *IEEE Transactions on Medical Imaging*, 22(1): 105-119, 2003.

Vincent L, Soille P. Watersheds in digital spaces: An efficient algorithm based on immersion simulations. *IEEE Transactions on Pattern Analysis and Machine Intelligence*, 13(6): 583-598, 1991.

Vincken KL, Koster ASE, Viergever MA. Probabilistic multiscale image segmentation. *IEEE Transactions Pattern Analysis and Machine Intelligence*, 19(2): 109-120, 1997.

Vrooman HA, Cocosco CA, van der Lijn F, Stokking R, Ikram MA, Vernooij MW, Breteler MMB, Niessen WJ. Multi-spectral brain tissue segmentation using automatically trained k-nearest-neighbor classification. *NeuroImage*, 37: 71-81, 2007

Wan S-Y, Higgins WE. Symmetric region growing. *IEEE Transactions on Image Processing*, 12(9): 1007-1015, 2003.

Wang J, Li X. Guiding ziplock snakes with a priori information. *IEEE Transactions on Image Processing*, 12(2): 176-185, 2003.

Weeks AR. Fundamentals of Electronic Image Processing. SPIE Optical Engineering Press, IEEE Press (copublishers), 1996.

Wei M, Zhou Y, Wan M. A fast snake model based on non-linear diffusion for medical image segmentation. *Computerized Medical Imaging and Graphics*, 28: 109-117, 2004.

Wells III WM, Grimson WEL, Kikinis R, Jolesz FA. Adaptive segmentation of MRI data. *IEEE Transactions on Medical Imaging*, 15(4): 429-442, 1996.

Wismuller A, Vietze F, Behrends J, Meyer-Baese A, Reiser M, Ritter H. Fully automated biomedical image segmentation by self-organized model adaptation. *Neural Networks*, 17: 1327-1344, 2004.

Withey D. Dynamic Edge Tracing: Recursive methods for medical image segmentation. Ph.D. dissertation, University of Alberta, Edmonton, Alberta, Canada, 2006.

Woolrich MW, Behrens TE. Variational Bayes inference of spatial mixture models for segmentation. *IEEE Transactions on Medical Imaging*, 25(10): 1380-1391, 2006.

Xia Y, Bettinger K, Shen L, Reiss AL. Automatic segmentation of the caudate nucleus from human brain MR images. *IEEE Transactions on Medical Imaging*, 26(4): 509-517, 2007.

Xu C, Prince JL. Snakes, shapes, and gradient vector flow. *IEEE Transactions on Image Processing*, 7(3): 359-369, 1998.

Xu M, Thompson PM, Toga AW. An adaptive level set segmentation on a triangulated mesh. *IEEE Transactions on Medical Imaging*, 23(2): 191-201, 2004.

Xue Z, Shen D, Karacali B, Stern J, Rottenberg D, Davatzikos C. Simulating deformations of MR brain images for validation of atlas-based segmentation and registration algorithms. *NeuroImage*, 33: 855-866, 2006.

Yang J, Duncan JS. 3D image segmentation of deformable objects with joint shape-intensity prior models using level sets. *Medical Image Analysis*, 8: 285-294, 2004.

Yushkevich PA, Piven J, Cody Hazlett H, Gimpel Smith R, Ho S, Gee JC, Gerig G. User-guided 3D active contour segmentation of anatomical structures: Significantly improved efficiency and reliability. *NeuroImage*, 31: 1116-1128, 2006a.

Yushkevich PA, Zhang H, Gee JC. Continuous medial representation for anatomical structures. *IEEE Transactions on Medical Imaging*, 25(12): 1547-1564, 2006b.

Zaidi H, Ruest T, Schoenahl F, Montandon M-L. Comparative assessment of statistical brain MR image segmentation algorithms and their impact on partial volume correction in PET. *NeuroImage*, 32: 1591-1607, 2006.

Zeng X, Staib LH, Schultz RT, Duncan JS. Segmentation and measurement of the cortex from 3-D MR images using coupled-surfaces propagation. *IEEE Transactions on Medical Imaging*, 18(10): 927-937, 1999.

Zhang D-Q, Chen S-C. A novel kernalized fuzzy c-means algorithm with application in medical image segmentation. *Artificial Intelligence in Medicine*, 32: 37-50, 2004.

Zhang Y, Brady M, Smith S. Segmentation of brain MR images through a hidden Markov random field model and the expectation-maximization algorithm. *IEEE Transactions on Medical Imaging*, 20(1): 45-57, 2001.

Zhou J, Rajapakse JC. Segmentation of subcortical brain structures using fuzzy templates. *NeuroImage*, 28: 915-924, 2005.

Zhou Y, Bai J. Atlas-based fuzzy connectedness segmentation and intensity nonuniformity correction applied to brain MRI. *IEEE Transactions on Biomedical Engineering*, 54(1): 122-129, 2007.

Zijdenbos AP, Forghani R, Evans AC. Automatic "pipeline" analysis of 3-D MRI data for clinical trials: Application to multiple sclerosis. *IEEE Transactions on Medical Imaging*, 21(10): 1280-1291, 2002.